Codeposition of Cu-Sn from Ethaline Deep Eutectic Solvent

Swatilekha Ghosh [a] and Sudipta Roy [a,*]

[a] School of Chemical Engineering and Advanced Materials, Merz Court, Newcastle University, Newcastle upon Tyne, United Kingdom

* Corresponding author: sudipta.roy@ncl.ac.uk

Abstract

Copper and tin have been co-deposited from choline chloride ethylene glycol based deep eutectic solvent (DES) containing $CuCl_2.2H_2O$ and $SnCl_2.2H_2O$. Initially, electrolyte formulation experiments were carried out containing different amounts of copper and tin at a brass cathode in a rotating cylinder Hull cell. It was found that metallic deposits containing copper and tin could be deposited from a DES containing 0.02 M $CuCl_2.2H_2O$ and 0.1 M $SnCl_2.2H_2O$. Polarization scans were carried out to determine the reduction potentials for individual metals and alloys. Anodic stripping voltammetry showed that Sn co-deposits with Cu at -0.36 V, at a lower over-potential than the tin reduction potential. Smooth and bright deposits of thicknesses up to 10 μm were obtained at a potential of -0.36 V or by using a current density of -0.87×10^{-3} A cm^{-2}. XRD analysis showed the formation of mainly Cu_3Sn and some Cu_5Sn_6. Our results suggest that Sn is co-discharged with Cu at potentials which is noble compared to the reduction potential of the individual metal.

Keywords: Copper-Tin Alloy, electrodeposition, Choline Chloride, Ethaline, Deep Eutectic Solvent

1. Introduction

Alloys of Cu and Sn find applications in wear and corrosion protection [1-5], electronic solders [6-12] and, more recently, for shape memory applications [13, 14] and lithium ion batteries [15-17]. The manufacturing process for Cu-Sn alloys employs traditional or automated metallurgical deposition processes [18], vapour deposition [19-21] as well as electrodeposition [1, 6, 12, 15-17, 22-34].

Of these techniques, arguably, the most energy efficient and economic method is electrodeposition using various acidic and alkaline aqueous solutions [1, 6]. However, many of these electrolytes employ cyanides [6] or addition agents [27-33] to improve issues related to deposit microstructure [34-37], which have come under regulatory scrutiny [38]. In addition, aqueous tin plating systems are encumbered with problems such as sludge formation and oxidation of Sn^{2+} to Sn^{4+} [1, 6, 30], which can only be avoided if non-aqueous systems are used. These difficulties have led the search for alternative electrolytes [28-31], such as ionic liquids (IL) [39-43].

An IL can be defined as "a mixture consisting solely of cations and anions with a melting point of 100°C and below" [41, 43]. Previous work on Cu-Sn alloy fabrication from ILs have mainly used 1-ethyl-3-methylimidazolium dicyanamide [EMI-DCA] [44, 45], trimethyl-n-hexylammonium [bis[trifluoromethyl]sulfonyl]amide [TMHA-Tf2N] [46, 47], 1-ethyl-3-methylimidazolium [bis[trifluoromethyl]sulfonyl]amide or [EMI-Tf2N] [48] melts. In the EMI-DCA based work Cu_3Sn nano-brushes were obtained at low current densities, but a detailed understanding of co-deposition was not the focus of that work.

In the TMHA-Tf2N based studies, researchers electrodeposited tin from an IL on to a copper substrate at a temperature between 150 - 190ºC. At these temperatures the IL remains stable, but copper from the substrate and plated tin inter-diffuse and form an alloy [46, 47]. The researchers termed this as the "reduction-diffusion" method. They formed an alloyed layer

of reasonably uniform thickness up to a depth of 4 μm [48] with an overall Sn content between 40 to 60 wt%. The deposits showed Cu_6Sn_5, Cu_3Sn and $Cu_{10}Sn_3$ intermetallic phases which depended on the applied potential, temperature of the IL and deposition time [47, 48]. The deposition of Cu and Sn could essentially be viewed as an inter-diffusion in the solid state.

One IL which may be used to deposit both copper and tin is the choline chloride (ChCl) based system [41, 49-58]. Researchers have deposited both copper [49-52], tin [53-56] and, more recently, Cu-Sn [57, 58] from this system. In addition, choline chloride is available in commercial quantities, is relatively inexpensive, and does not require special chemical purification methods. The other attractive properties are low volatility [41, 59], viscosity [60, 61] and reasonably high solubility of both metals [62]. ChCl based ILs are not true ionic liquids, and are termed deep eutectic solventss (DES). A DES consists of $C_5H_{14}NOCl$ (choline chloride), along with a hydrogen bond donor (HBD) such as CH_4N_2O (urea), $C_2H_2O_4$ (oxalic acid), $C_3H_8O_3$ (glycerol), $CH_2(COOH)_2$ (malonic acid), or $C_2H_6O_2$ (ethylene glycol) which exhibit a deep eutectic point [41]. Metals are deposited from anhydrous or hydrated metal salts as well as oxides which are dissolved into this DES.

While considerable effort has been expended to deposit Cu-Sn alloys [43-47, 57, 58] from different kind of ionic liquids, a comprehensive understanding for Cu-Sn co-deposition is lacking. The most systematic study on alloy electrodeposition from ionic liquids (or room temperature molten salts) has been carried out using chloraluminate salts by Hussey and co-workers [63, 64]. They analysed the deposition behaviour for a number of Al-based alloys, such as Cu-Al, Ni-Al and Co-Al plated from BMIM-$AlCl_3$ melts [65]. They found that in the presence of copper and nickel, discharge of Al proceeded at potentials more anodic than its reduction potential. In addition, only the rate of deposition is dependent on the concentration of copper species, but the composition of the deposit was independent. This deposition

behaviour was attributed to the gain in surface energy due to alloy formation [65]. The reaction mechanism for the co-deposition of the two metals is given by:

$$x\ Cu^{+}\ (solv) + 4(1-x)\ Al_2Cl_7^{-} + (3-2x)e^{-} \leftrightarrow Cu_xAl_{(1-x)} + 7(1-x)AlCl_4^{-}$$

In this regard they can be compared to under-potential deposition [65] since Al deposition does not at these potentials.

Alloy deposition behaviour using ChCl-based ILs, however, is not as well understood. For example, researchers have demonstrated the feasibility of Sn-Ni deposition from choline-chloride urea and ethylene glycol [66], and reported Sn content as high as 72% in the deposit along with other inter-metallics and oxide. However, this study focused on determining currents where deposition could be achieved [67], and an in-depth analysis of the co-deposition process was not pursued. A later work on Ni-Zn alloy deposition using choline-chloride urea melts revealed that nickel is the major component in the deposit [68]. A recent paper on Cu-In deposition from ChCl-urea melt investigated the electrochemical and co-deposition behaviour of the individual metals and their alloys [69]. Their study showed that the electrochemical behaviour was complex and, depending on the concentration of individual metal ions and electrode potential, Cu, Cu_2In, CuIn or In could be deposited. The authors remarked that this behaviour was indicative of formation of an alloy (or inter-metallic) which was most energetically favourable. These different findings show that further understanding of alloy deposition from DES is required.

The aim of this work was to develop a deeper understanding of co-deposition behaviour using ChCl-based DES. For this present study, ethaline, a DES obtained using a 1:2 choline chloride and ethylene glycol mixture (ChCl-2EG), has been chosen to deposit a Cu-Sn alloy. In all deposition experiments hydrated salts were dissolved in the DES, since they are easily available in market and widely used in the plating industry. In order to achieve our aim, a set of electrochemical deposition experiments using different electrolyte formulations and a

rotating cylinder Hull cell (RCH) have been carried out. A separate set of polarisation experiments were performed to determine the electrochemical behaviour. In these experiments, a Pt rotating disk electrode (RDE) was used. Electrochemical co-deposition behaviour was compared against single metal deposition to determine if alloys were formed at under or over-potentials. Anodic stripping voltammetry (ASV) coupled with energy dispersive x-ray (EDX) analysis was performed to verify if metallic deposits were obtained. Finally, co-deposition of Cu-Sn alloys was carried out on a low-carbon steel RDE to achieve 5 to 10 μm deposit thickness. The deposit morphology, elemental composition and crystalline structure were determined using standard materials analyses.

2. Experimental

2.1 Melt Preparation

The ethaline melt was prepared by mixing analytical grade choline chloride [$C_5H_{14}NOCl$] and ethylene glycol [$C_2H_6O_2$] in a 1:2 ratio, which is referred to as ChCl-2EG throughout this text. Choline chloride as received from Sigma-Aldrich (> 98% purity) was used without further purification. This mixture was kept in a thermostatic heater at 40°C and stirred for 24 hours until it formed a colourless liquid. The mixture was then stored in an airtight glass bottle to minimize the interaction with atmosphere. Subsequently, 0.10 M $SnCl_2.2H_2O$ (Sigma-Aldrich) was added to the melt, which reflects the solubility limit of $SnCl_2.2H_2O$ in ethaline [56]. Thereafter 0.02, 0.04 or 0.10 M of $CuCl_2.2H_2O$ was added to the tin salt-ethaline DES. This means that the Cu:Sn ratio were 1:5, 1:2.5 and 1:1 in the different DES. These solutions are termed as 1:5 ChCl-2EG, 1:2.5 ChCl-2EG, and 1:1 ChCl-2EG, respectively, and are listed in Table 1. Finally, the melt was stirred for 2 hours until it formed a homogeneous solution.

The use of hydrated copper and tin chloride introduces water in the DES, but this is not necessarily detrimental to the electrodeposition process. Since choline and glycol are hygroscopic, it is difficult to avoid water entering the DES. Secondly, it has been shown that oxygen evolution can stop glycol from reacting at the anode [70]. Thirdly, using hydrated salt allows one to have control over the amount of water being introduced into the DES (typically, 8% to 13%) provides a more stable deposition system [49, 56]. In addition, it has been shown that Cu and Sn species present in hydrated and dehydrated DES are the same for water content up to 40% [71-73]. These species are also presented in Table 1.

2.2 Apparatus

2.2.1 Electrolyte Formulation Experiments:

Prior to plating, it is important to determine the solvent formulation which allows the co-deposition of metals. Therefore, a series of plating experiments were carried out where different compositions of ethaline, i.e. 1:5 ChCl-2EG, 1:2.5 ChCl-2EG, and 1:1 ChCl-2EG were used. These experiments were carried out using a rotating cylinder Hull cell (Rota-Hull) [74, 75].

A Rota-Hull consists of a rotating cylinder cathode, which is separated from the anode by an insulator. It is designed with a particular geometry which allows it to mimic the current distribution of a Hull cell [74]. The use of a rotating cylinder allows one to control mass transfer to the cathode by simply changing the rotation speed [74]. Therefore, this apparatus allows one to deposit metals or alloys at a variety of current densities in a single experiment under controlled mass transfer conditions [75]. An Autolab HT Rota-Hull cell (Eco Chemie B.V) employing a 0.6 cm diameter cylindrical rotating brass electrode and Pt mesh as counter electrode was used in the current study. The rotation speed of the working electrode was fixed

145 at 600 rpm and the operating temperature was 22 ± 2 °C. Full detail of the RCH apparatus and
146 the rationale for choice of current density and the rotation speed is provided in the
147 *supplementary materials section* of this paper.

148

149 2.2.2 *Polarisation, Anodic Stripping Voltammetry and Codeposition Experiments*

150 Polarisation experiments were carried out in a standard three-electrode cell using a platinum
151 rotating disc electrode (RDE) (Radiometer Analytical), with a Pt mesh as counter electrode.
152 The cell was a jacketed glass vessel, and was maintained at a constant temperature of 25ºC
153 using a recirculation system. A silver wire served as a quasi-reference electrode, which has
154 been established to be stable in these DES under a wide variety of conditions [43, 49, 55,56].
155 Potential scans were performed using a computer controlled μ-Autolab instrument in a scan
156 range of -1.0 V to +1.0 V and the scan rate was set at 0.01 V s^{-1}.

157 Codeposition experiments were performed in a low-carbon steel disc of 0.9 cm diameter
158 (i.e. 0.64 cm^2) using an RDE apparatus. This disc was detachable from RDE which assisted in
159 surface preparation and deposit characterisation. Potentiostatic deposition was performed using
160 the Autolab instrument using a three-electrode system, and galvanostatic plating was carried
161 out using a PL320 constant power supply (Thurlby-Thandar) using a two-electrode set up. In
162 all galvanostatic experiments, the potential of the working electrode was monitored against the
163 reference in order to ensure that the potential of the electrode corresponded to that of the
164 potentiostatic co-deposition experiments. The cell arrangement for these experiments can be
165 found in our earlier publications [49, 56, 61].

166

167 *2.2.3 Deposit Characterisation*

In order to measure deposit thickness, the substrate surface was masked with lacquer before deposition. After deposition the lacquer mark was removed using acetone, and the thickness of the deposit was obtained using a Olympus BX41 confocal optical microscope. Four measurements were performed to reduce errors in thickness measurement. A Hitachi S2400 Scanning Electron Microscope fitted with an Oxford Instruments Isis 200 Ultra-Thin Window X-ray Detector (for EDX analysis) was used to ascertain deposit morphology and composition.

A PANalyticalX'Pert Pro MPD, powered by a Philips PW3040/60 X-ray generator and fitted with an X'Celerator were used for x-ray diffraction measurements. The instrument was operated in a scan range of 5° to 99° (in 2θ scan mode) with a step size of 0.0334°, a nominal time per step of 100 seconds, and using CuKα radiation of 1.54 keV. The scans were performed in 'continuous' mode using the X'Celerator RTMS detector. The phase identification of the obtained scans were carried out by the X'Pert accompanying software program PANalytical High Score Plus in combination with the ICDD Powder Diffraction File 2 database (1999), the American Mineralogist Crystal Structure Database (March 2010) and the Crystallography Open Database (September 2011; www.crystallography.net) system.

2.3 Procedure

2.3.1 Electrolyte Formulation Experiments

In order to obtain a wide range of current density in the Rota-Hull experiments, the applied current density was varied between -1.0 x 10^{-3} and -1.7 x 10^{-3} A cm^{-2}. The deposition time was set at 180 min to achieve a deposit thickness of at least 3 µm, so that an EDX analysis could be carried out. Since the current density at the Rota-Hull changes from the top to the bottom, the current at different parts of the cylinder were calculated. The procedure for these calculations

is shown in the *supplementary material section.* The maximum and minimum nominal current densities at the bottom and top of the cylinder were determined to be -2.9 x 10^{-3} A cm^{-2} and -0.15 x10^{-3} A cm^{-2} (*cf. supplementary material*). At the end of a plating experiment the brass substrates were dismounted and were sectioned into four parts. The composition of each section was determined by EDX to check for alloy formation.

2.3.2 Polarisation and Anodic Stripping Voltammetry Experiments

Once the electrolytes useful for co-deposition of the copper and tin were determined, polarisation experiments were carried out using those formulations to further examine their electrochemical behaviour. The RDE rotation rate was fixed at 220 rpm and the scan rate was 0.01 V s^{-1}. Polarization scans were also carried out using individual metals, to investigate the individual metal reduction and stripping in the above scan range, using same scan rate, RDE speed and temperature.

A further set of anodic stripping voltammetry (ASV) were carried out to probe the potentials at which individual metals or intermetallic compounds were deposited and dissolved. In these experiments deposition was carried out at potentials between -0.33 V to -0.5 V for 3 to 10 min duration, which was followed by stripping voltammetry in a scan range between -0.5 to +1.0 V at a scan rates 0.01 V s^{-1}. Other experimental parameters were identical to those for the polarisation experiments.

2.3.3 Co-deposition Experiments

Cu-Sn deposits were obtained by either galvanostatic or potentiostatic deposition by depositing at potentials of -0.36 V or a current of -0.87 x 10^{-3} A cm^{-2}. The choice of potential and current was based on the requirement that a metallic deposit needed to be plated. Notably the applied

current lay in the range of current densities explored in the electrolyte formulation experiments (*cf. 2.3.1*). The RDE rotation rate was fixed at 220 rpm in order to achieve same mass transfer conditions as that obtained at the Rota-Hull system, and deposition time was set at 240 min to obtain a deposit of around 10 µm thick. At the end of each experiment the plated disc was washed with water and acetone and detached from its holder for material analysis. The thickness, composition, morphology and crystalline structure of deposits were determined using standard analytical techniques.

3. Results

3.1 Electrolyte Formulation Experiments

Figure 1 shows the deposits obtained from 1:1 ChCl-2EG, 1:2.5 ChCl-2EG, and 1:5 ChCl-2EG, which correspond to cylinders A, B and C. Sample A shows a smooth red deposit, indicative of only copper deposition. This was confirmed by EDX analysis of all four sections of the deposit. The applied current for this deposition experiment was -1.7×10^{-3} A cm^{-2} which means that the current density over the cylinder varied between -4.2×10^{-3} to -0.25×10^{-3} A cm^{-2}. These data show that tin cannot be co-deposited with copper using this electrolyte formulation within this current range.

Samples B and C show deposits which change in colour from red to grey which is indicative of Cu as well as Sn deposition. The applied current density was to -1.0×10^{-3} and -1.2×10^{-3} A cm^{-2}, respectively. The lower currents are simply due to the lower copper deposition rate corresponding to a lower copper reduction current, since Sn is assumed to be plated at the same rate as before. Visually, the grey colour is observed in the portions where the current density is high, i.e. primarily in sections 3 and 4 for cylinder B and sections 2 to 4 for cylinder C. EDX analysis of these samples showed Sn content ranging 3 to 12 at% and 4 to 11 at% for

239 cylinders B and C, respectively. These data show that Cu-Sn alloys can be co-deposited from
240 these two electrolytes for a current range between -0.15 x 10^{-3} and -3.0 x 10^{-3} A cm^{-2}. The range
241 of alloy composition is larger for 1:2.5 ChCl-2EG and the deposit is smoother; in this regard
242 this particular DES is most appropriate for Cu-Sn co-deposition.

243 EDX analysis for sections 1 and 2 also showed the presence of oxygen (21 at%) and
244 carbon (13 at%) for sample B, with still higher values for sample C. However, in sections 3
245 and 4, where the plating current is lowest, the content of oxygen and carbon was found to be
246 lower. This showed that as the deposition current is raised the amount of Sn, O and C would
247 increase. Although higher Sn contents would be achieved at high currents (or potentials), the
248 deposit would contain oxygen and carbon. Therefore, in order to determine if Sn content could
249 be increased by changing the ratio of copper and tin in the electrolyte, a set of deposition
250 experiments was also carried out with 0.01 M $CuCl_2.2H_2O$ - 0.1 M $SnCl_2.2H_2O$ in the DES (i.e.
251 10:1 ChCl-2EG). Although the Sn content in the deposit increased to 80 at%, the deposit was
252 powdery and therefore unsuitable for alloy deposition.

253 From these experimental findings it is clear that co-deposition of Cu-Sn is achievable
254 in a range of electrolyte formulations which contain 1:2.5 ChCl-2EG and 1:5 ChCl-2EG. Since
255 the maximum amount of hydrated $SnCl_2.2H_2O$ that can be dissolved in ChCl-2EG is 0.1 M,
256 this fixes the amount of copper that can be added to the IL. In this case it also appears that
257 lower current densities are preferable for metallic alloy deposition, especially since deposit
258 properties deteriorate and oxygen and carbon are incorporated in the deposit.

259

260 *3.2 Polarization and Anodic Stripping Experiments*

Figure 2(a) shows the typical polarization scans at a Pt electrode for 1:5 ChCl-2EG, and 1:2.5 ChCl-2EG. The figure shows that reduction commences at a potential of -0.33 V, and reaches a plateau current. A second wave commences at a potential -0.5 V, and a second mass transfer limiting current is observed at a potential just above -0.6 V. In the reverse sweep three clear stripping currents are observed. These stripping processes started at a potential of -0.5 V, -0.3V and +0.4 V as marked by A, B and C in Figure 2(a). When the copper concentration in the DES is increased, as is the case for 1:2.5 ChCl-2EG, peak A becomes smaller and peak B becomes larger. The small oxidation peaks appearing to the right of both A and B stripping peaks for the 1:5 has been observed during electrodeposition from aqueous systems and is attributed to formation of Cu-Sn interfacial phases [31].

Typical polarisation scans in Pt electrode for ethaline containing individual metals, *i.e.*, $CuCl_2.2H_2O$ (0.02 M and 0.04 M) and $SnCl_2.2H_2O$ (0.1 M) are presented in Figures 2(b) and 2(c), respectively. Figure 2(b) shows that the first reduction from Cu^{2+} to Cu^{+} occurs at +0.45 V. The second reduction peak, corresponding to Cu^{+} reducing to Cu is observed at a potential of -0.33 V. A mass transfer limiting current is observed beyond -0.45 V. Oxidation peaks are observed as the scan is reversed. When the copper content in the electrolyte is doubled, the plateau current is also augmented by the same factor, showing mass transfer control [49].

Figure 2(c) shows that Sn is reduced at -0.38 V, an over-potential slightly more cathodic than that for the reduction of Cu^{+} to Cu. A mass transfer limiting current is again observed at potentials below -0.5 V. The reverse sweep shows two stripping peaks: one at a -0.38 V and another at -0.17 V. In an earlier work [56] these attributed to the oxidation of two different Sn species present in the electrolyte.

Comparing the individual metal deposition peaks it is clear that both metals can co-reduce in the potential region below -0.38 V and they can both be governed by mass transfer at potentials below -0.5 V. The first and second stripping peaks (A and B in Figure 2(a)) could

correspond to the dissolution of single or both metals, since it is possible to electro-oxidise either a single metal or an alloy phase at these potentials. The decrease in peak height of A with increase in copper content in the DES is indicative that this peak may be associated with tin or tin-rich phases. Peak B, on the other hand, increases when copper content in solution is increased, which indicates that it may correspond to Cu or Cu-rich phases. The third stripping peak (C) can be attributed to the oxidation of Cu^{+} to Cu^{2+} [49], since Sn should have been completely stripped at these potentials. Further anodic stripping voltammetry was carried out to determine which metals or phases are stripped in these regions for the 1:2.5 ChCl-2EG electrolyte, because this electrolyte formulation produced the best deposits.

3.3 Anodic stripping experiments

Table 2 lists the potentials used for ASV analysis for a 1:2.5 ChCl-2EG electrolyte, which covers the potential range within which either one or both metals are expected to co-deposit. Figure 3 shows the corresponding stripping voltammograms. Depending on the applied potential for deposition, two or three different stripping peaks are observed. At a potential of -0.33 V, peaks are observed corresponding to the positions where peaks B and C were located in the polarisation measurements (*cf.* Figure 2(a)). These are indicated by B' and C' in Figure 3. An EDX analysis for the deposit showed that the deposit contained only Cu, as would be expected at these potentials.

As the potential is lowered to -0.36 V, the two peaks are again visible at their respective positions, and the total charge under the stripping peaks is higher. An EDAX analysis showed that both copper and tin are present in this deposit. The charge under peak B' was similar to that observed for -0.33 V, but the charge under peak C' is increased. This shows that Cu and Sn are co-reducing at -0.36 V, and that the deposit contains significant amounts of copper.

Interestingly, Sn is deposited at -0.36 V, which is nobler compared to the reduction potential of Sn as an individual metal (*cf.* Figure 2(c)). The co-reduction of Sn could be due to the fact that alloy formation is energetically more favourable.

As the deposition potential was lowered further (i.e., -0.4 V, -0.45 V and -0.5 V) a third stripping peak, A', is observed. The position of A' is similar to that for peak A shown in Figure 2(a). This peak grew more prominent as the potential is lowered, while the charge corresponding to peak B' remained nearly constant. This indicates that Sn is deposited at potentials below -0.4 V and that peak A in Figure 2(a) is associated with a Sn phase. This is consistent with the reduction potential for Sn (below -0.38 V) obtained in the polarisation data. The small oxidation peak appearing to the right of A' may be due to the presence of an inter-phase between the two Sn-containing phases [34, 35].

EDX analysis of these deposits showed the presence of oxygen and carbon, the quantities of which are listed in Table 2. For deposits obtained at -0.5 V, 9 at% of chlorine was also found along with oxygen and carbon. The presence of these impurities are in agreement with our earlier work on copper deposition, where carbon and chlorine were detected [49], which is attributed to the breakdown of the DES itself. The current findings confirm that low deposition potentials are inappropriate for metallic Cu-Sn co-deposition, since impurities can be incorporated in the deposit. Therefore, further co-deposition experiments were carried out using potentials of -0.36 V or the current corresponding to this potential, i.e. -0.87×10^{-3} A cm^{-2}.

3.4 Codeposition experiments

Figure 4(a) and (b) show scanning electron micrographs of a typical deposit obtained potentiostatically (at -0.36 V) or galvanostatically (using a current of -0.87×10^{-3} A cm^{-2}). As

observed in the micrographs, the deposits are dense and reasonably smooth. It may be expected that the choice of substrates can affect the deposit morphology and microstructure. However, the deposits on the steel substrate using the RDE were similar to those obtained using the RotaHull experiments for cylinders B and C in the region where co-deposition of Cu and Sn occurred.

The deposit composition, as determined EDX analysis, showed the Sn content to be 17 at% for the potentiostatic experiments and 13 at% for the galvanostatic experiments, respectively. The copper content in the deposit was found to be approximately 83 at% (error in analysis being $\pm$10%). Elements such as C, O or Cl were not detected.

Deposition was also carried out just below and just above -0.36 V to determine the sensitivity of alloy composition to electrochemical parameters. In agreement with the ASV findings, deposits at potentials of -0.34 V contained only Cu. At deposition potentials of -0.355 V, a lower amount of Sn (*ca*. 2 to 5 at%) was found. For the corresponding galvanostatic experiment carried out at a current density of -0.64 x 10^{-3}A cm^{-2}, a similar alloy composition was obtained. At a potential of -0.375 V or the corresponding galvanostatic experiment (-0.095 x 10^{-3}A cm^{-2}) increased amounts of oxygen (*ca*. 20 to 30 at%) was detected. These findings also show that metallic deposits can be attained within a very narrow range of current or potentials and that alloy composition is very sensitive to the applied potential.

The film growth rate at a potential of -0.36 V was determined to be 0.035 ± 0.003 μm min^{-1}. Deposit thicknesses up to 10 μm could be attained by increasing plating time without compromising deposit quality. The current efficiency for deposition, calculated using charge balances, were found to be 90%. Gravimetric measurements of current efficiency were found to be in excellent agreement with charge balance data, *i.e.* 92%.

357 The morphology of the deposited alloy is similar to that observed for Cu-Sn alloys
358 deposited from aqueous electrolytes without addition agents or under laboratory conditions [24,
359 28, 31, 76] and other ILs [45-47, 57]. The grains near the electrode surface are small, typically
360 of the order of 1 μm. The micrograph shows the presence of many nuclei near the substrate
361 interface demonstrating the importance of nucleation in the initial stages of deposition. As the
362 deposit grows, only some of the grains grow larger in the longitudinal direction. This is very
363 similar to electrodeposited Cu-Sn alloys from aqueous systems from MSA electrolytes in bench
364 scale systems [31].

365

366 *3.5 Phase Analysis*

367 The XRD diffractograms for the Cu-Sn alloys deposited on a stainless steel substrate for the
368 same DES composition and potential as those for Figure 4 are shown in Figure 5. The different
369 peaks of the diffractogram correspond to mainly orthorhombic Cu_3Sn [77] and few others for
370 hexagonal Cu_6Sn_5 [78]. Separate phases for Cu and Sn are absent. When Cu-Sn were co-
371 deposited from other ILs, phases similar to Cu_6Sn_5, Cu_3Sn and $Cu_{10}Sn_3$ [45, 47] were found,
372 similar to those obtained from aqueous electrolytes [6, 28, 31, 79, 80].

373 Since the predominant phase is Cu_3Sn, one would expect an atomic ratio of 75:25 for
374 Cu:Sn in the deposit. The EDX data showed a ratio of 80:20 atomic percent for Cu:Sn. The
375 EDX and XRD results, can be considered to be in broad agreement, given that the error in EDX
376 measurement could be as high as 10%. If there is any excess Cu in the deposit, the absence of
377 a peak associated with it may be due to the fact that it is either a disordered structure or it is
378 dissolved in the Cu_3Sn phase.

For powder Cu_3Sn samples the ratio of intensity (in %) for (021):(002):(121):(231):(331) peaks are 70:100:100:70:70 [77]. The intensity ratios estimated from Figure 5 is 100:12:35:15:10, which shows a polycrystalline structure of mostly (021) orientation. On closer inspection a doublet is observed for the (121) peak. This can be due to presence of $K\alpha_1$ and $K\alpha_2$ components in the incident and diffracted beams from the Cu source as monochromatization was not carried out during the XRD scan.

The zoomed picture of the doublet and other intense peaks, *i.e*. (021) and (231) is presented in Figure 6. The average primary crystallite size was determined using these peaks and the Scherrer equation [81]. Crystallite size was determined to be 21 ± 10 nm, against a value of 30 to 100 nm for the aqueous systems [82]. The strain contribution was determined using the same diffraction peaks using the Williamson-Hall method [49, 83]. The strain value was 0.012 ± 0.005, somewhat lower than that for the individual metals plated from the same DES [49, 56].

4. Discussion

Our findings indicate that alloy deposition from ChCl-2EG produces Cu-Sn compounds, depending on the electrolyte chosen. This is similar to findings of Dale *et.al.* for Cu-In [69], and Zn-Ni [67] deposition from ChCl based DES. The deposition of Sn proceeds at more noble potentials compared to the reduction potential of the individual metal. This is similar to the case observed for the deposition of Al alloys obtained from imidazolium-based ILs [65]. In this regard, ChCl DES seems to exhibit similarities with imidazolium systems.

There are different principles of electrochemical co-deposition which have mainly been tested for aqueous systems and based on over-potential methodologies [84]. However,

402 underpotential deposition of alloys or phases is also possible [85] from aqueous systems. In
403 addition, more recently additional models for electrochemical deposition of alloys based on
404 electrolyte speciation [86] and energetics in the solid state have been proposed [85]. It is
405 interesting to compare the current Cu-Sn deposition system in view of these alternative
406 mechanisms.

407 The electrolyte formulation experiments show that Cu-Sn deposition occurs from a
408 DES containing a particular amount of individual metals. If the concentrations of the individual
409 metals were changed, co-deposition did not occur, or that deposit properties were poor. This
410 may be indicative of electroactive species formed in DES which contains Cu and Sn in the ratio
411 of 3:1, which would lead to the formation of a single compound, Cu_3Sn. Such a system would
412 follow the model of Younes and Gileadi [86] where speciation in solution influences the
413 deposition product.

414 The second possibility is that Cu_3Sn is formed due to the lowering of overall energy in
415 the solid state due to alloy formation. This is plausible as it has been found that Sn is depositing
416 at potentials more positive to that required for Sn reduction from DES containing only Sn salt.
417 In this case, the two metals may deposit (nearly) independently, but the thermodynamics of the
418 deposit controls the phases formed, as has been suggested for the imidazolium systems [65].
419 While this does not preclude the formation of an electroactive species as described in the
420 previous paragraph, it does not require it. A differentiation between the two processes will
421 require the identification of multi-metal species in DES as well as a careful assessment of
422 energies of alloy formation, which may be useful avenues of further research.

423 One interesting aspect arising from the result is the unusually high content of oxygen
424 and carbon in the deposited material. These occur at higher currents and potentials, thereby
425 restricting the metal and alloy deposition rate. This observation is similar to those obtained

426 previously for copper and tin deposition by our group [49, 56]. There can be a number of
427 reasons for the presence of these elements in deposits: entrapment of electrolyte, co-deposition of
428 oxides and embedment of material can all occur.

429 However, in our earlier work we found that current efficiencies were between 84-95%
430 [49, 56] These measurements were verified using gravimetric, cuolometric as well as thickness
431 measurements. Since the content of oxygen and carbon is relatively high, electrolyte
432 entrapment or embedment of electrolyte within the deposit would have resulted in
433 disagreement between these measurements. In addition, the morphology of more porous
434 material (Cu and Sn [49, 56]) contained less oxygen and chlorine. These elements could also
435 arise from the deposition of oxides or chloride compounds, but these were never detected in
436 our XRD measurements in this work or our earlier work or by any researchers.

437 Figure 7 shows the polarisation data for ChCl-2EG at a Pt RDE. These data show the
438 reaction involving the solvent and show the electrochemical window of ethaline. The figure
439 shows that the IL breaks down below a potential of -0.7 V, as reported previously [30, 46].
440 However, low currents are observed at -0.4 V, indicating that some degree of break down
441 begins at relatively low potentials. Both Cu, Sn and Cu-Sn are depositing at these potentials,
442 and carbon and oxygen detected in the deposits may be arising from the breakdown of the
443 solvent, which has also been reported by other researchers [70]. Although the currents recorded
444 on Pt are low, it is possible that the process is favoured during Cu-Sn deposition, which will
445 be studied further by our group.

446

447 **5. Conclusions**

Copper and tin have been successfully co-deposited from a choline chloride ethylene glycol based deep eutectic solvent (DES). It was found that metallic deposits containing copper and tin can be deposited from a DES containing 0.04 M $CuCl_2.2H_2O$ and 0.1 M $SnCl_2.2H_2O$, i.e. 1:2.5 ChCl-2EG. Anodic stripping voltammetry showed that Sn co-deposits with Cu at -0.36 V, at a potential more noble than the tin reduction potential in the DES. EDX analysis showed that only Cu and Sn are co-deposited at -0.36 V. At higher over-potentials, oxygen, carbon and chlorine were also present. XRD analysis showed the formation of mainly Cu_3Sn and some Cu_5Sn_6 at -0.36 V. Our results suggest that Sn is co-discharged with copper at potentials which are noble (compared to its reduction potential) because alloy formation is energetically favoured.

Acknowledgement

Swatilekha Ghosh acknowledges NUIPS and ORSAS scholarship from Newcastle University.

References

1. M. Jordan, Electrodeposition of Tin-Lead Alloys, in: M. Schlesinger, M. Paunovic (Eds.), Modern Electroplating, 5th Edition, John Wiley & Sons, Hoboken, New Jersey, 2010.
2. R. Schaefer, J. B. Mohler, U.S. Patent, 1,373,488 (1921).
3. G. C. Pratt, International Materials Reviews, 18 (1973) 62.
4. A. Knödler, C. J. Raub, E. Raub, Metalloberfläsche, 38 (1984) 496.
5. B. Subramanian, S. Mohan, S. Jayakrishnan, Surf. Coat. Technol., 201 (2006) 1145.
6. W. E. G. Hansal, Pulse Plating of Tin and its Alloys, in: W.E.G. Hansal and S. Roy (Eds.), Pulse Plating, Leuze Verlag, Bad Saulgau, 2012.
7. H. M. Batten, C. J. Welcome, U.S. Patent 1,970,548 (1934).
8. S. W. Baier, D. J. MacNaughtan, U.S. Patent 2,511,395 (1950).
9. G. J. Jackson, R. Durairaj, N. N. Ekere, Proceedings of Electronics Manufacturing Technology Symposium, 2002. IEMT 2002.
10. Y. Qin, G. D. Wilcox, C. Liu, Electrochim. Acta, 56 (2010) 183.
11. D. Padhi, S. Gandikota, H. B. Ngyuyen, C. McGruik. S. Ramanathan, J. Yahalom, G. Dixit, Electrochim. Acta, 48 (2003) 935.

12. J.-T. Huang, P.-S. Chao, H.-J. Hsu, S.-H. Shih, Materials Science in Semiconductor Processing, 10 (2007) 133.
13. M. Ceylan, R. Zengin, Journal Materials Processing Technology, 97 (2000) 148.
14. M. Yuasa, K. Kajikawa, M. Hakamada, M. Mabuchi, Materials Letters, 62 (2008) 4473.
15. N. Tamura, R. Ohshita, M. Fujimoto, S. Fujitani, M. Kamino, I. Yonezu (2002) J. Power Sources, 107 (2002) 48.
16. F.-S. Ke, L. Huang, J.-S. Cai, S.-G. Sun, Electrochim. Acta, 52 (2007) 6741.
17. W. Pu, X. He, J. Ren, C. Wan, C. Jiang, Electrochim. Acta, 50 (2005) 4140.
18. Z. S. Karim, J. Martin, International Symposium on Microelectronics, Baltimore, MD, 2001, pp. 581-587.
19. P. Doppelt, T. H. Baum, Chemistry of Materials, 12 (1995) 2217.
20. S. Dhabal, T. B. Ghosh, Appl. Surf. Science, 211 (2003) 13.
21. R. Z. Hu, Y. Zhang, M. Zhu, Electrochim. Acta, 53 (2008) 3377.
22. S. D. Beattie, J. R. Dahn, J. Electrochem. Soc., 150 (2003) C457.
23. B. Kim, T. Ritzdorf, J. Electrochem. Soc., 150 (2003) C53.
24. G. A. Finazzi, E. M. de Oliveira, I. A. Carlos, Surf. Coat. Technol., 187, (2004) 377.
25. D. Radovic, Plat. Surf. Finish., 76 (1989) 52.
26. A. N. Correia, M. X. Facanha, P. de Lima-Neto, Surf. Coat. Technol., 201 (2007) 7216.
27. S. Arai, Y. Funaoka, N. Kaneko, N. Shinohara, Electrochemistry, 69 (2001) 319.
28. C. T. J Low, F. C. Walsh, Surf. Coat. Technol., 202 (2008) 1339.
29. C. T. J. Low, F. C. Walsh, Electrochim. Acta, 53 (2008) 5280.
30. N. Pewnim, S. Roy, Trans. Inst. Metal Finishing, 89 (2011) 206.
31. N. Pewnim, S. Roy, Electrochim. Acta, 90 (2013) 498.
32. I. A. Carlos, E. D. Bidoia, E. M. J. A. Pallone, M. R. H. Almeida, C. A. C. Souza, Surf. Coat. Technol., 157 (2002) 14.
33. A. Survila, Z. Mockus, S. Kanapeckaite, V. Jasulaitiene, R. Juskenas, Electrochim. Acta, 52 (2007) 3067.
34. L. F. Senna, S. L. Díaz, L. Sathler, J Appl. Electrochem., 33 (2003) 1155.
35. K. N. Pu, Materials Chemistry and Physics, 46 (1996) 217.
36. W. J. Boettinger, C. E. Johnson, L. A. Bendersky, K.-W. Moon, M.E. Williams, G.R Stafford, Acta Mater., 53 (2005) 5033.
37. T. N. Vorobyova, V. P. Bobrovskaya, V. V. Sviridov, Metal Finishing, 95 (1997) 14.
38. M. Tomkiewicz, Environmental Aspects of Electrodeposition, in: M. Schlesinger, M. Paunovic (Eds.), Modern Electroplating, 5th Edition, John Wiley & Sons, Hoboken, New Jersey, 2010
39. F. Endres, S.Z.E. Abedin, Phys. Chem. Chem. Phys. 8 (2006) 2101.
40. H. Ohno (Ed.), Electrochemical Aspects of Ionic Liquids, John Wiley & Sons, New York, 2005.
41. F. Endres, A. P. Abbott, D. R. MacFarlane (Eds.), Electrodeposition from Ionic Liquids, WILEY-VCH, Weinheim, 2008.
42. H. Olivier-Bourbigou, L. Magna, D. Morvan, Applied Catalysis A: General, 373 (2010) 1.
43. A. P. Abbott, K. J. McKenzie, Phys. Chem. Chem. Phys. 8 (2006) 4265.
44. Y.-T. Hsieh, I.-W. Sun, Electrochem. Commun., 13, (2011) 1510.
45. Y.-T. Hsieh, T.-I. Leong, C.-C. Huang, C -S. Yeh, I.-W. Sun, Chem. Commun., 46, (2010) 484.
46. T. Katase, R. Kurosaki, K. Murase, T. Hirato, Y. Awakura, Electrochem. Solid-State Lett., 9 (2006) C69.

47. K. Murase, R. Kurosaki, T. Katase, H. Sugimura, T. Hirato and Y. Awakura, J. Electrochem. Soc., 154 (2007) D612.
48. K. Murase, A. Ito, T. Ichii and H. Sugimura, J. Electrochem. Soc., 158, (2011), D335.
49. S. Ghosh, S. Roy, Surf. Coat. Technol., 238 (2014) 165.
50. C. D. Gu, Y. H. You, X. L. Wang, J. P. Tu, Surf. Coat. Technol., 209 (2012) 117.
51. T. Tsuda, L. E. Boyd, S. Kuwabata, C. L. Hussey, J. Electrochem. Soc., 157 (2010) F96.
52. A.-M. J. Popescu, V. Constantin, M. Olteanu, O. Demidenko, Rev. Chim., 62 (2011) 626.
53. S. Salome, N. M. Pereira, E. S. Ferreira, C. M. Pereira, A. F. Silva, J. Electroanal Chem., 703 (2013) 80.
54. C. D. Gu, Y. J. Mai, J. P. You, J. P. Tu, J. Power Sources, 214 (2012) 200.
55. A. P. Abbott, G. Capper, K. J. McKenzie, K. S. Ryder, J. Electroanal. Chem., 599 (2007) 288.
56. S. Ghosh, S. Roy, Journal of Material Science and Engineering: B, 190 (2014) 104.
57. A. Alhaji, "Electrodeposition of Alloys from Deep Eutectic Solvents", PhD Thesis, University of Leicester, Leicester, UK (2011).
58. S. Ghosh, "Electrodeposition of Cu, Sn and Cu-Sn Alloy from Choline Chloride Ionic Liquid", PhD Thesis, Newcastle University, Newcastle-upon-Tyne, UK (2013).
59. W. Simka, D. Puszczyk, G. Nawrat, Electrochim. Acta, 54 (2009) 5307.
60. A. P. Abbott, G. Capper, D. L. Davies, R. K. Rasheed, P. Shikotra, Inorg. Chem., 44 (2005) 6497.
61. S. Ghosh, K. S. Ryder, S. Roy, Trans. Ins. Met. Finishing, 92 (2014) 41.
62. A. P. Abbott, G. Capper, D. L. Davies, R. K. Rasheed, V. Tambyrajah, Chem. Commun., 2003, 70.
63. B. J. Tierney, W. R. Pitner, J. A. Mitchell, C. L. Hussey, G. Stafford, J. Electrochem. Soc., 145 (1998) 3110.
64. Q. Zhu, C.L. Hussey, J. Electrochem. Soc., 148 (2001) C395.
65. Q. Zhu, C.L. Hussey, G.R. Stafford, J. Electrochem. Soc., 148 (2001) C88.
66. A. Florea, L. Anicai, S. Costovici, F. Golgovici, T. Visan, Surf. Interface Anal., 42 (2010) 1271.
67. L. Anicai, A. Petica, S. Costovici, P. Prioteasa, T. Visan, Electrochim. Acta, 114, (2013) 868.
68. H. Y. Yang, X. W. Guo, X. B. Chen, S.H. Wang, G. H. Wu, W. J. Ding, N. Birbilis, Electrochim. Acta, 63 (2012) 131.
69. J. C. Malaquias, M. Steichen, M. Thomassey, P. J. Dale, Electrochim. Acta, 103 (2013) 15.
70. K. Haerens, E. Matthijs, K. Binnemans, B.-V. der Bruggen, Green Chem., 11 (2009) 1357.
71. P. de Vreese, N. R. Brooks, K. V. Hecke, L. V. Meervelt, E. Matthijs, K. Binnemans, R. V. Deun, Inorg. Chem., 51 (2012) 4972.
72. G. Li, D. M. Camaioni, J. E. Amonette, Z. C. Zhang, T. J. Johnson, J. A. Fulton, J. Phys. Chem. B, 114 (2010), 12614.
73. M. Currie, J. Estager, P. Licence, S. Men, P. Nockemann, K.R. Seddon, M. Swadźba-Kwaśny, C. Terrade, Inorg. Chem., 52 (2013) 1710.
74. C. Madore, "Analyse Théorique et Réalisation Pratique de Nouveaux Dispositifs Expérimentaux Pour L'étude de la Distribution des Courants Partiels Lors d'électrodeposition D'alliages" These No. 1189, Ecole Polytechnique Federale de Lausanne (1993).
75. C. Madore, D. Landolt, C. Haßenpflug, J.A. Hermann, Plat. Surf. Finish., 82 (1995) 36.

578 76. Y. Sürme, A. A. Gürten, E. Bayol, E. Ersoy, J. Alloy Compounds, 485 (2009) 98.
579 77. [ICDD reference code 00-006-0621], I. Isajcev, Zh. Tekh. Fiz. 17 (1947) 829.
580 78. [ICDD reference code 00-047-1575], B. Peplinski, Federal Inst. for Material Research
581 and Testing, Berlin, Germany, *Private Communication* (1995).
582 79. W.M. Tang, A.-Q. He, Q. Liu, D.G. Ivey, Trans. Nonferrous Met. Soc. China. 20 (2010)
583 90.
584 80. H.-C. Shin, M. Liu, Adv. Funct. Mater., 15 (2005) 582.
585 81. P. Scherrer, *Göttinger Nachrichten Gesell.* 2 (1918) p 98. (as referred to in B.D. Cullity,
586 S.R. Stock, Elements of X-ray Diffraction, 3rd Ed, Prentice Hall, 2001, pp. 167-171).
587 82. C. Han, Q. Liu, D.G. Ivey, Electrochim. Acta, 54 (2009) 3419.
588 83. G. K. Williamson, W. H. Hall, Acta Metall., 1 (1953) 22.
589 84. D. Landolt, Electrochim. Acta, 39 (1994) 1075.
590 85. Y. D. Gamburg and G. Zangari, Theory and Practice of Metal Electrodeposition,
591 Springer, New York (2011), pp. 219-225.
592 86. O. Younes-Metzler, L. Zhu, E. Gileadi, Electrochim. Acta, 48 (2003) 255.
593

Figure Captions

Figure 1: Electroplated cylinders from RCH cells for different ethaline DES formulations. (A) 1:1 ChCl-2EG, (B) 1:2.5 ChCl-2EG, and (C) 1:5 ChCl-2EG. The cylinders were sectioned into four parts which are marked in the figure. The current density across each of these sections were as follows: **Pt1**: $2.5i_{Avg}$, **Pt2**: $1.0i_{Avg}$, **Pt3**: $0.3i_{Avg}$, **Pt4**: $0.15i_{Avg}$, where i_{Avg} is the applied current.

Figure 2: Cyclic voltammograms for co-deposition from **(a)** —1:5 ChCl-2EG ; – – -1:2.5 ChCl-2EG at a Pt RDE rotating at 220 rpm. The scan rate is 0.01 V s^{-1} and scan direction is shown by the arrows. Voltammetry for individual metal deposition **(b)**—0.02 M $CuCl_2.2H_2O$; – – 0.04 M $CuCl_2.2H_2O$ **(c)** — 0.1 M $SnCl_2.2H_2O$ using the same experimental conditions.

Figure 3: Anodic stripping voltammograms for deposits plated from with 1:2.5 ChCl-2EG at Pt RDE, at potentials listed in Table 2 ; —0.33 V, – – 0.36 V, — 0.40 V, — 0.45 V —0.5 V. Stripping was carried out at a rotation speed of 220 rpm and a scan rate 0.01 V s^{-1}.

Figure 4: SEM micrographs of Cu-Sn deposits on stainless steel substrates from 1:2.5 ChCl-2EG electrolyte: (a) applied potential of - 0.36 V and (b) a current density of -0.87 x 10^{-3} A cm^{-2} . The total time of deposition was 4 hours and the RDE speed was 220 rpm. (c) Typical deposit cross-section after plating for 4 hours.

Figure 5: XRD diffractograms of individual metals and alloy plated from ChCl-2EG DES. Trace (A) Cu plated from DES containing 0.04 M $CuCl_2.2H_2O$, (B) Cu-Sn deposited using the conditions shown in Figure 4(c), and (C) Sn plated from DES containing 0.1 M $SnCl_2.2H_2O$.

Figure 6: Zoom of the most intense peaks for Cu_3Sn from the XRD diffractogram shown in Figure 5 which were used to calculate grain size and strain. The peaks are (a) (021), (b) (121), and (c) (231).

Figure 7: Potential scan showing electrochemical window of ethaline at Pt RDE, scan rate 30 mV/s, 25 °C at an RDE; (....) 100 rpm, (——) 2500 rpm.

Table 1

Nomenclature, composition and metal salts used in the experiments. The speciation of copper and Sn in the IL are also shown.

Choline Chloride (M)	**Ethylene Glycol (M)**	**Copper** $CuCl_2.2H_2O$ (M)	**Tin** $SnCl_2.2H_2O$ (M)	**Nomenclature**
1.0	2.0	0.02	0.1	1:5 ChCl-2EG
1.0	2.0	0.04	0.1	1:2.5 ChCl-2EG
1.0	2.0	0.1	0.1	1:1 ChCl-2EG
Speciation in DES		$[CuCl_3]^-$ $[CuCl_4]^{2-}$	$[SnCl_3]^-$ $[Sn_2Cl_5]^-$	

Table 2

Potentials, charge under stripping peaks and EDX analysis for electrodeposits used in the ASV analysis for a 1:2.5 ChCl-2EG DES.

Potential (V)	**Calculated charge under stripping peaks** (C)			**Carbon** content as per EDX analysis (at%)	**Oxygen** content as per EDX analysis (at%)
	Peak A	Peak B	Peak C		
- 0.33	-	0.50	0.04	-	-
- 0.36	-	0.45	0.23	-	-
- 0.40	0.03	0.40	0.10	12	20
- 0.45	0.09	0.40	0.14	23	30
- 0.50	0.16	0.50	0.05	26	40

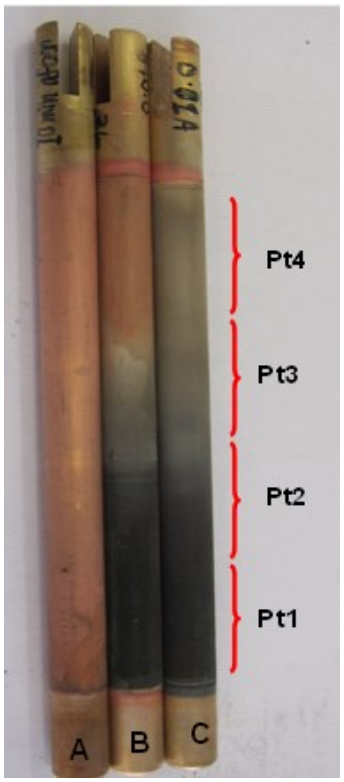

Figure 1: Electroplated cylinders from RCH cells for different ethaline DES formulations. (A) 1:1 ChCl-2EG, (B) 1:2.5 ChCl-2EG, and (C) 1:5 ChCl-2EG. The cylinders were sectioned into four parts which are marked in the figure. The current density across each of these sections were as follows: **Pt1**: $2.5i_{Avg}$, **Pt2**: $1.0i_{Avg}$, **Pt3**: $0.3i_{Avg}$, **Pt4**: $0.15i_{Avg}$, where i_{Avg} is the applied current.

649

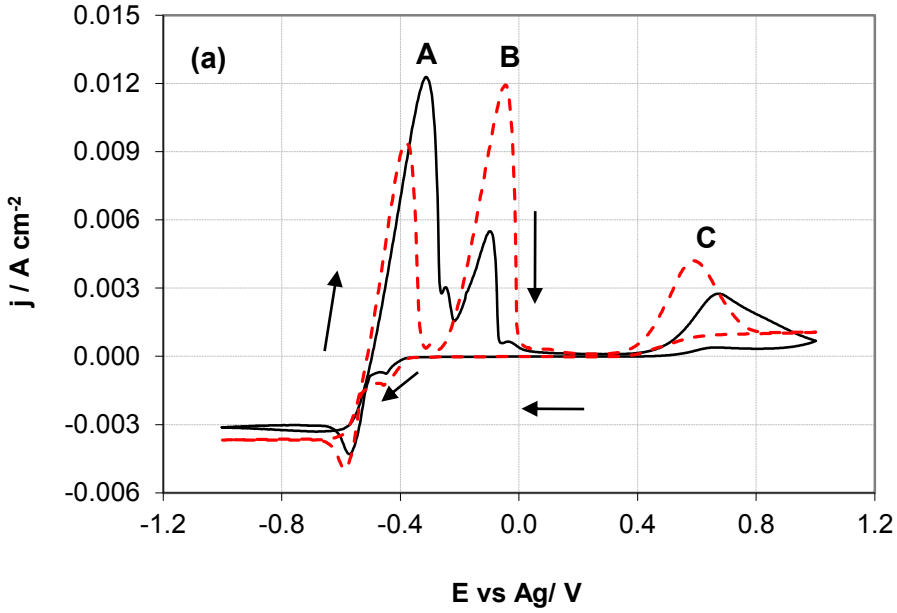

650

651

652

653

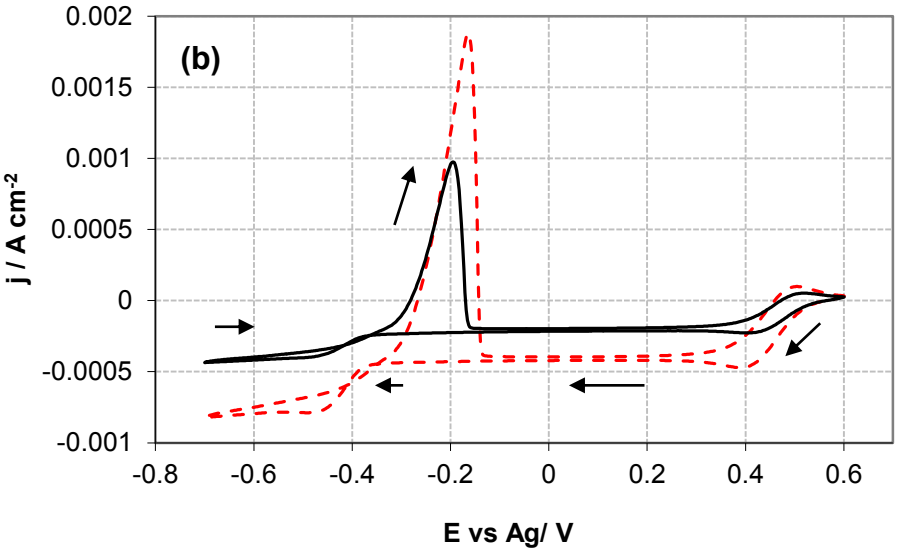

654

655

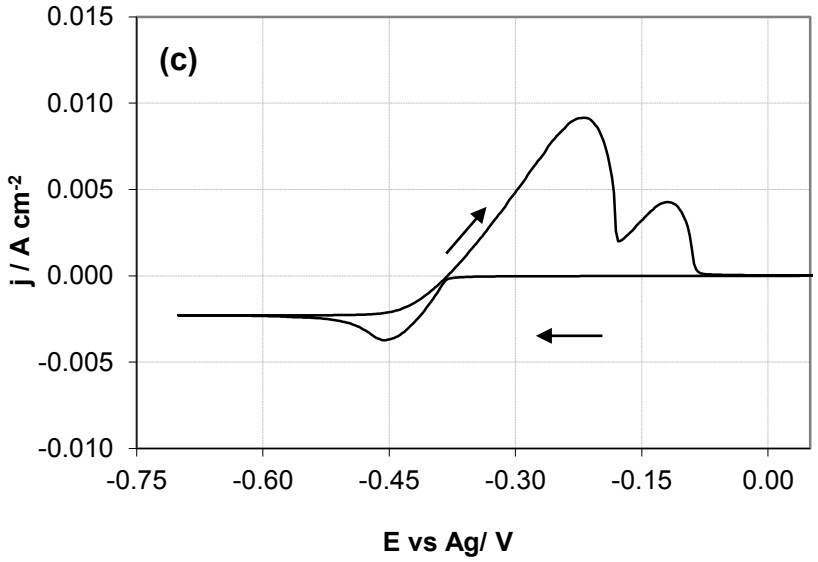

Figure 2: Cyclic voltammetry data at a Pt RDE rotating at 220 rpm. The scan rate is 10 mV/s and scan direction is shown by the arrows.
(a) —1:5 ChCl-2EG ;– – -1:2.5 ChCl-2EG ; (b)—0.02 M $CuCl_2.2H_2O$; – –0.04 M $CuCl_2.2H_2O$ (c) — 0.1 M $SnCl_2.2H_2O$

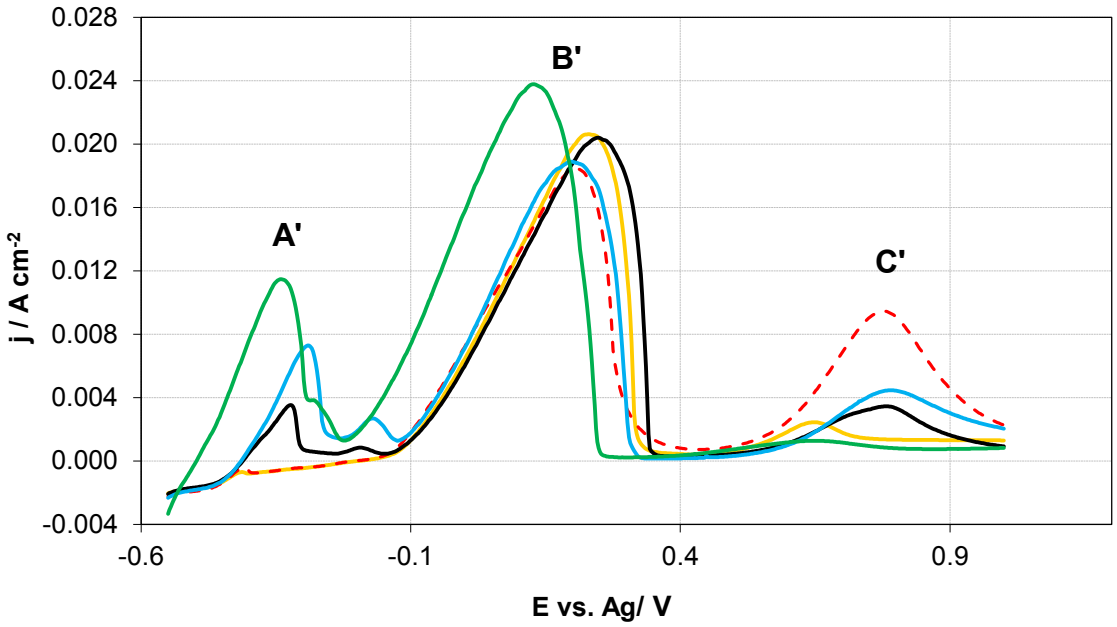

Figure 3 : Anodic stripping voltammetry with 1:2.5 ChCl-2EG at Pt RDE at a rotation speed of 220 rpm and scan rate 10 mV/s. Potentials used : (—)0.33 V, (– –)0.36 V, (—)0.4 V, (—)0.45 V, (—)0.5 V

681

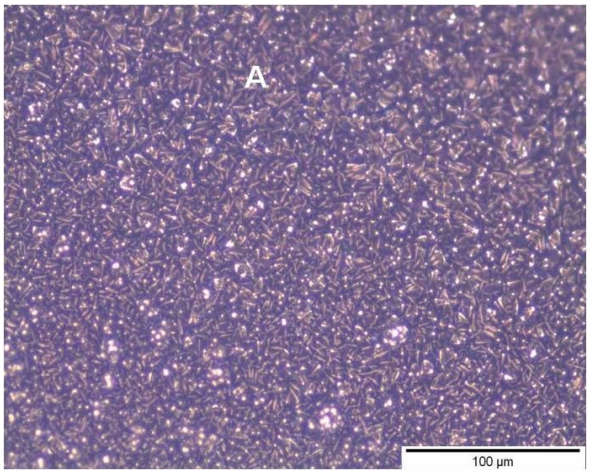

682

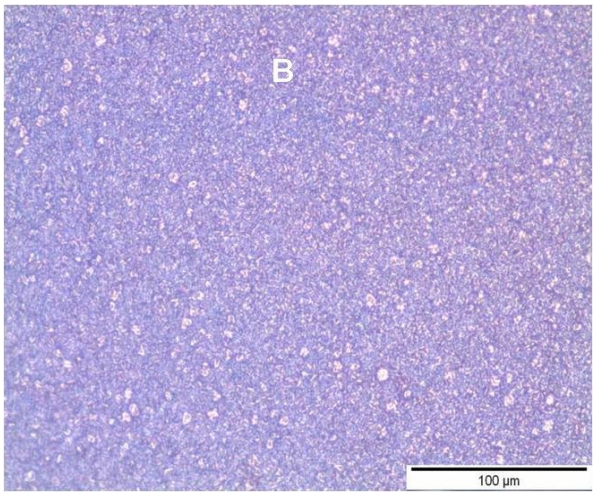

683

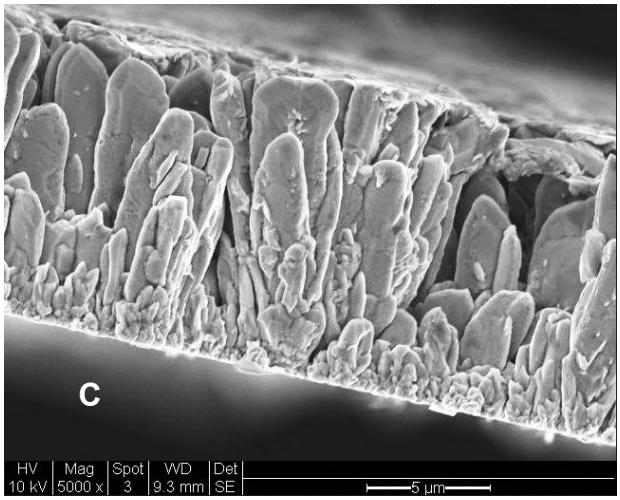

684

685 **Figure 4:** SEM micrographs of Cu-Sn deposits on stainless steel substrate from 1:2.5 ChCl-
686 2EG electrolyte: (a) applied potential of - 0.36 V and (b) a current density of -0.87 x 10^{-3} A cm^{-2}
687 . The total time of deposition was 4 hours and the RDE speed was 220 rpm. (c) Typical deposit
688 cross-section after plating for 4 hours.
689
690

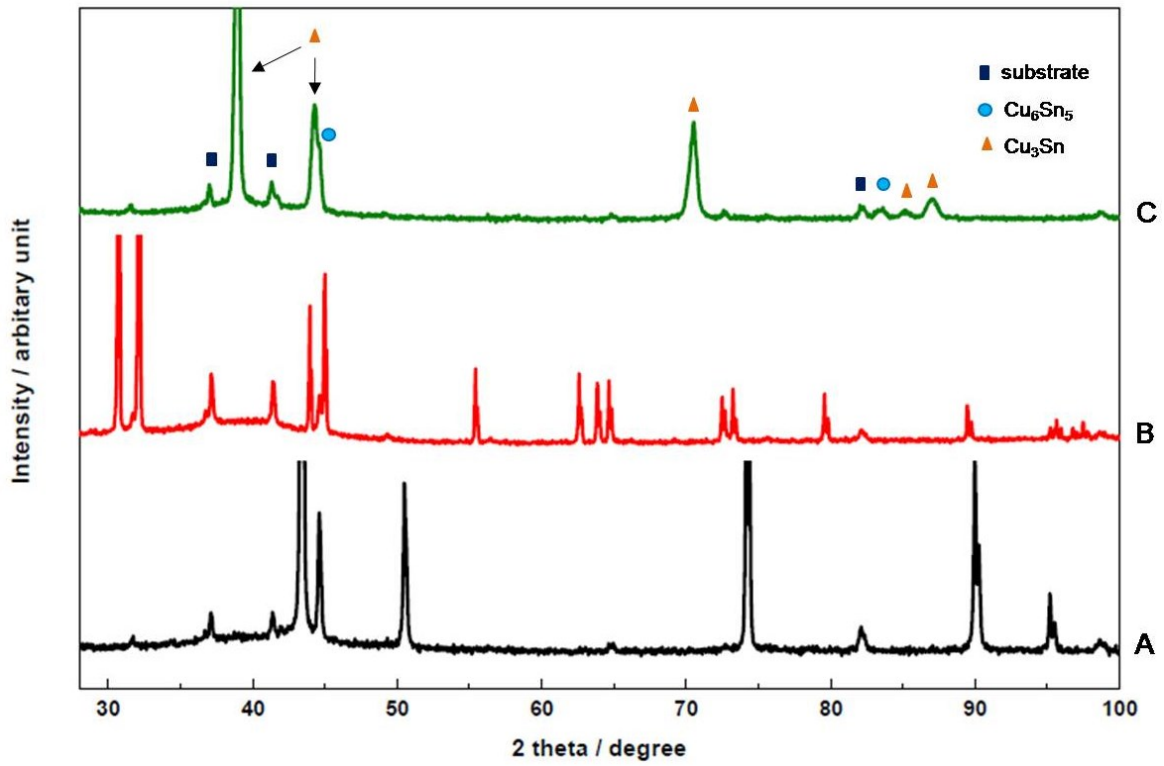

691

692

693 **Figure 5**: XRD diffractograms of individual metals and alloy plated from ChCl-2EG DES.
694 Trace (A) Cu plated from DES containing 0.04 M $CuCl_2.2H_2O$, (B) Cu-Sn deposited using the
695 conditions shown in Figure 4(c), and (C) Sn plated from DES containing 0.1 M $SnCl_2.2H_2O$.

696

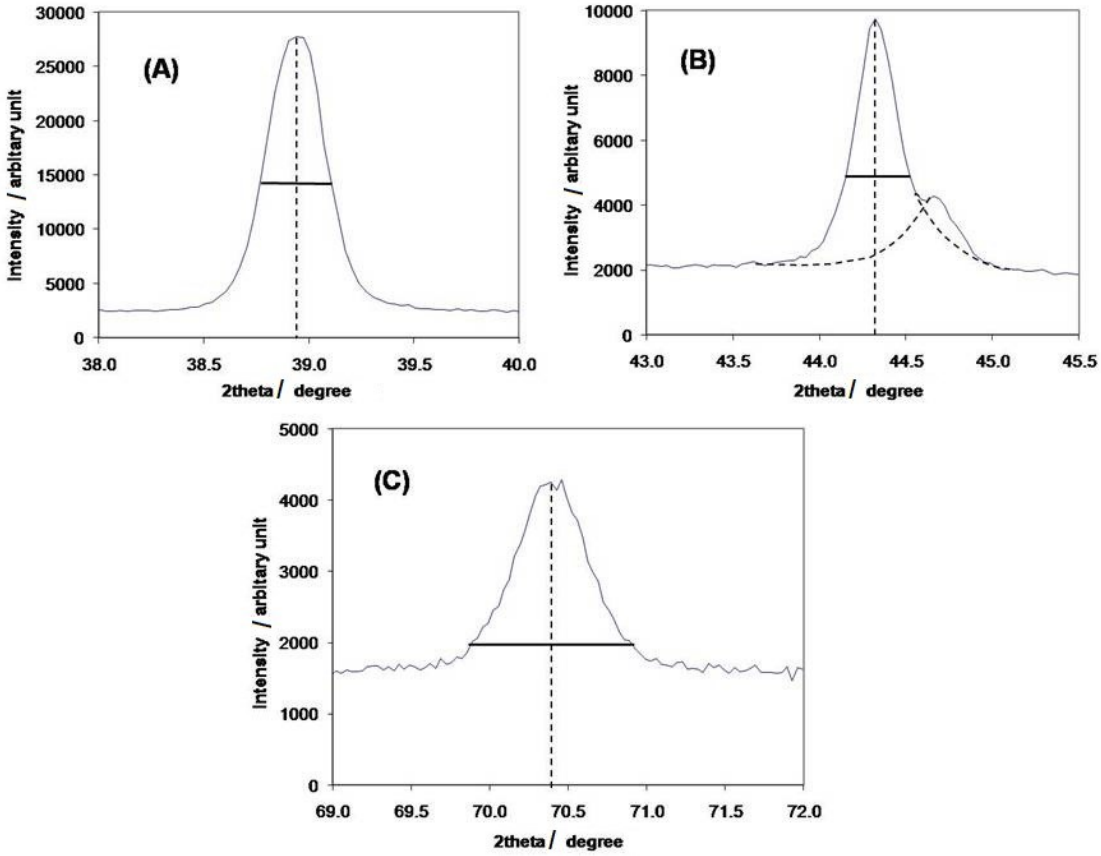

Figure 6: Zoom of the most intense peaks for Cu_3Sn from the XRD diffractogram shown in Figure 5 which were used to calculate grain size and strain. The peaks are (a) (021), (b) (121), and (c) (231).

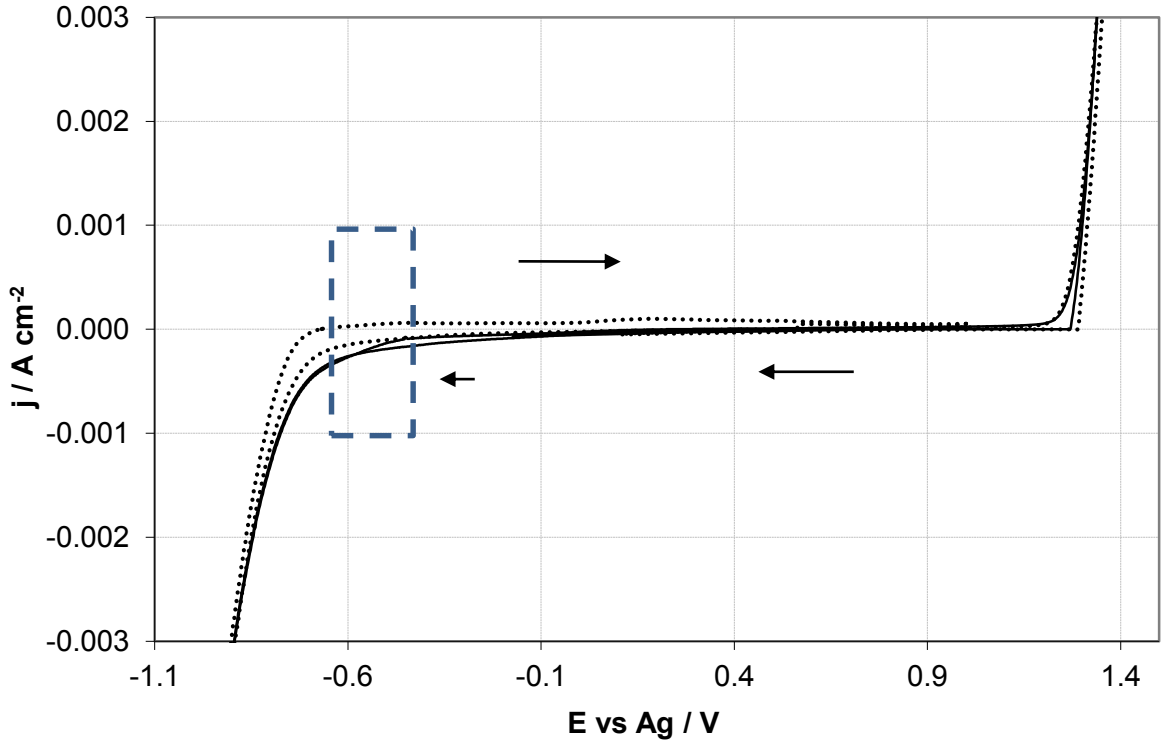

Figure 7: Potential scan showing electrochemical window of ethaline at Pt RDE, scan rate 30 mV/s, 25 °C at an RDE; (....) 100 rpm, (——) 2500 rpm.